International Journal of Engineering Trends and Technology
ISSN: 2231 – 5381 / https://doi.org/10.14445/22315381/IJETT-V70I6P235
Volume 70 Issue 6, 337-348, June 2022

Performance Evaluation of A PV- Powered Alkaline Water Electrolyzer for Sustainable Green Hydrogen Production

Nand Kishore Singh[1], Seema Saxena[2], Vinod Krishna Sethi[3]

[1]*SoEEM, RGPV, Bhopal, M.P, India*
[2]*EX Deptt. UIT-RGPV, Bhopal, M.P, India*
[3]*R.K.D.F. University, Bhopal, M.P, India*

nandkishore_70@yahoo.co.in

Received: 26 April 2022 Revised: 08 June 2022 Accepted: 11 June 2022 Published: 29 June 2022

Abstract **-** *Hydrogen is a potential candidate that can serve as a large-scale and long-term storage medium for renewable energy sources. Alkaline Water Electrolysis (AWE) is the only established and technically matured technology for the large-scale production of clean hydrogen. However, finding cost-effective and sustainable materials to design the critical components of alkaline electrolysis cells is still one of the pressing challenges of this technology. This paper presents an experimental study for hydrogen production by alkaline water electrolysis employing austenitic stainless steel electrodes (SS316, SS316L & SS310). The study at RGPV Bhopal intends to evaluate the field performance of AWE under examination by independently using the three sets of electrodes with normal and modified surface morphologies. The impact of surface morphology modification on the cell current density and hydrogen gas evolution rate is experimentally investigated for the three sets of electrodes. The electrolyzer is powered by an array of 0.9kW$_p$amorphous silicon thin film(aSi-TF) P.V. modules. Integrating the aSi-TFPV array and the electrolyzer is done via a DC-DC converter developed for power conditioning and control.*

Results reveal that surface morphology modification improves cell current and rate of experimental hydrogen production for all the three austenitic S.S. electrode specimens, with SS310 electrodes exhibiting better cell current values & gas production rates overSS316 & SS316L electrodes.

Keywords **-** *Green Hydrogen, Alkaline Water Electrolysis(AWE), Austenitic Stainless-Steel Electrodes, Surface Morphology, aSi- TFPV modules, DC-DC Converter.*

1. Introduction

The inherent sporadic nature of renewable energy resources poses multifold challenges to electric power systems' performance, reliability, and stability [1,2]. This exigency mandates an urgent need to develop storage mechanisms for RES. Besides being efficient and sustainable, it must be capable of large-scale and long-term renewable energy storage [3].

Hydrogen produced by the electrochemical splitting of water using electricity from RES can be an excellent energy storage medium due to its extremely high purity (99.9999%) levels, near-zero carbon emission, and simplicity of the electrolysis process[5,8,9]. As for this particular experimental study, the focus will be on utilizing solar P.V. electricity as the primary feedstock for water electrolysis since it is an established, safer, efficient & utility-scale clean power generation technology enabling straight conversion of sunlight into D.C. electricity[6]. Although three principal electrochemical reactor technologies are available for water splitting (e.g., AWE, PEM & SOE), only alkaline water electrolysis (AWE) is technically matured enough to offer the prospects of scalability for large-scale production of hydrogen to fulfill the ultimate demands of hydrogen usage, specifically for critical applications such as power generation and urban transportation[5]. Besides, alkaline water electrolysis systems offer the advantage of simplicity, robustness, and modularity as well. For water electrolysis to become a truly sustainable technology for clean hydrogen generation, the selection of materials for the design and fabrication of the vital components of the water electrolyzers (electrode systems, in particular) should be a reasonable trade-off between the electro-catalytic performance of the material, and it's price & availability. However, finding low-cost electrode materials that are both efficient and durable is one of the impending challenges for AWE systems[7].

As a consequence, high production costs of hydrogen through the electrochemical route are the principal hindering factor in the widespread deployment of water electrolysis technologies for hydrogen production[6,12,22]. It can be attributed to two main reasons: the high capital costs of electrolyzers[12]and the high electric energy consumption during water electrolysis,

leading to low process efficiencies[22,24]. The former reason becomes pronounced particularly for small electrolyzers with hydrogen production capacities up to 100 LPD [12]. The electrode system represents one of the critical components in a water electrolysis cell. The electro-catalytic performance of electrodes is a key parameter in determining the system efficiency of the water electrolyzer. Specific materials for electrodes with excellent electro-catalytic properties, low electrical resistance, and high corrosion resistivity, such as nickel, gold &platinum, etc., are ideal choices for electrode materials. However, these materials are either noble metals that are scarcely available and are very expensive [13,14]

Some of the notable experimental studies undertaken using electrodes made up of stainless steel to study the performance of alkaline water electrolyzer are discussed here briefly. Lavorante et al. [19]have experimentally studied the performance of SS316 electrodes, which were treated chemically to increase their active surface area. Nassar et al. [17] have attempted to study the corrosion behavior of some conventional stainless steels with cylindrical geometries at different temperatures. Colli et al. [16], to search for non-precious materials for electrodes with better corrosion resistance & electro-catalytic properties, have used Raney- Nickel as cathode and SS316L as an anode in a monopolar AWE configuration at 75ºC. Ramirez et al. [15] have used three different stainless plates of steel (viz. SS316, SS304 & SS430) to study the hydrogen evolution reaction(HER) with NaOH& KOH as electrolytes. Zeng & Zhang[23] have used Nickel electrodes mechanically polished with emery papers of different grain sizes to modify and improve their surface profile. They have also used the electrochemical deposition technique's chemical coating of Ni & Co.

However, most previous works have employed grid-assisted laboratory-scale D.C. supplies for powering the water electrolysis cells. Little attention has been paid to the use of electricity directly from RES (Solar P.V., Wind) as a primary feedstock for the water electrolyzer to study the real-time effects of the fluctuations in the electric power supply(due to the intermittency of RES) on the operational performance of the electrolysis cell. Further, in most of the previous research, important process parameters, especially electrolyte concentration and current densities, were maintained at very low or moderate levels.

This paper investigates the performance of an alkaline water electrolysis cell (a monopolar, tank-type 2-electrode system) designed and fabricated for this study. Three different austenitic stainless steel electrodes (SS316, SS310 & SS316L) having plate geometry & normal as well as modified surface topology are deployed sequentially to study the key performance parameters of the cell, i.e.,, electric energy consumption & rate of hydrogen production. A low-cost approach is adopted to modify the electrode plate's surface topology to increase its active surface area[23]. The cell module is specially selected from transparent acrylic material to facilitate a visual study of the formation, rise, and subsequent accumulation of larger gas bubbles on the top of the electrolyte bath, a phenomenon which becomes pronounced particularly at higher values of current densities.

2. Description of Experimental Apparatus & Method

The block diagram for the experimental test set-up used for this study is presented in fig. 1 & the main components are discussed.

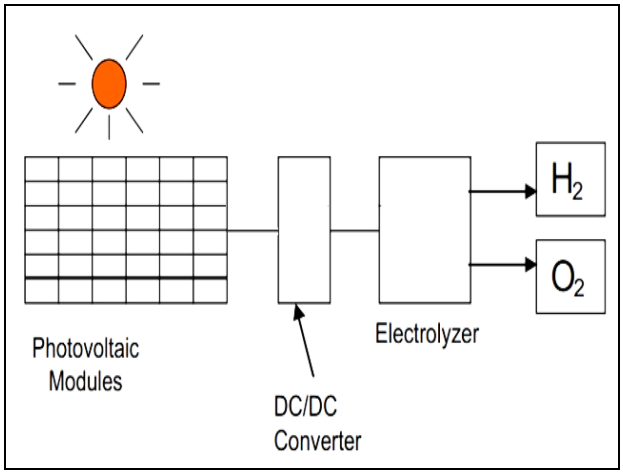

Fig. 1 Block diagram for the test set-up

2.1. P.V. Generator

The primary feedstock (D.C. supply) for the alkaline water electrolysis cell was derived from a 0.9kW$_p$ P.V. array comprising 9 Nos. of a-Si TFPV modules (SCHOTT Solar AG, ASI-100 series, 100Wp each) electrically connected in series.

Fig. 2 P.V. Generator

2.2. Power conditioning system

The integration of 0.9 kW$_p$ amorphous silicon thin film(a-SiTF) P.V. array with the AWE is performed by DDO (DC-DC converter optimization) technique[25] using a DC-DC converter for power conditioning and control. The converter employs a push-pull topology and is designed & developed to operate at an unregulated input D.C. voltage & a highly fluctuating, solar irradiance-dependent input photocurrent (from the P.V. generator) and deliver a regulated output of 0-6VDC & 0-50ADC to the load.

Fig. 3 Power Conditioning System

2.3. Electrolyzer

A small electrolysis cell was designed for this study which comprised of an air-tight chamber made of chemical & corrosion resistant transparent acrylic material with dimensions of 175mm(L)× 80mm (B) ×182mm (H). Zirfon-Perl® UTP 500membrane (thickness 0.5mm) (supplied by M/s Agfa Gevaert AG, Mortsel, Belgium) is a separating medium between the electrodes. The dimensions of the electrodes are 120mm×140mm & the thickness is 1.5mm. The electrodes are mechanically separated at a pre-defined gap but electrically isolated from each other using PVDF stud bolts and washers. The outlet points for the electrode cables and the gas pipes were carefully sealed using epoxy putty sealant material to prevent the escape of gases. Hydrogen was measured using a calibrated burette, whereas oxygen was released into the atmosphere.

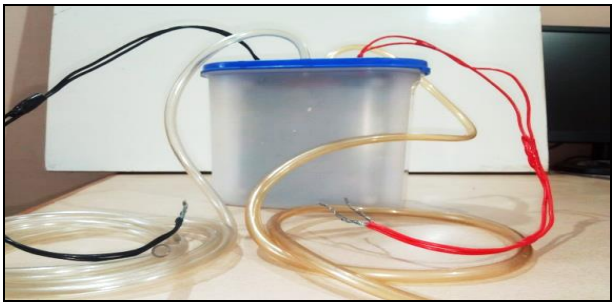

Fig. 4 Electrolyzer

2.4. Gas measurement system

The hydrogen produced was measured by water displacement using a 50 ml graduated burette ('J-sil' make) installed vertically on a retort stand with the help of HDPE fisher clamps (Polylab make).

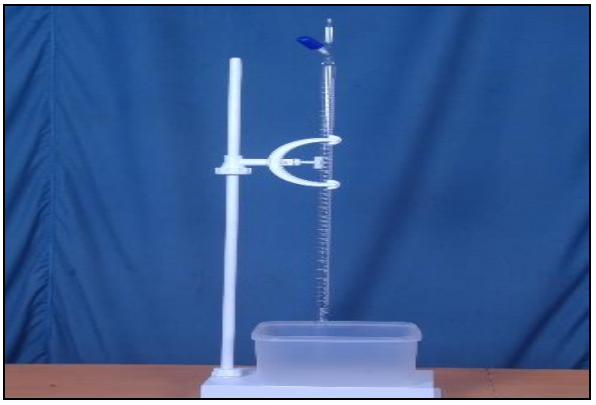

Fig. 5 Gas Measurement System

2.5. Chemicals

Potassium hydroxide solution is used as an electrolyte for this study. To prepare the KOH solution of the required concentration, a mass of dry potassium hydroxide flakes (Molychem 85%) was weighed using a precision analytical balance. It was then dissolved in a specific volume of de-ionized water (ULTRAPUR-TG®, 6µ S cm-1 at 18ºC).

Fig. 6 Chemicals (De-ionized water & KOH flakes)

Fig. 7 Experimental test set-up

3. Experimental Section

The experimental test set-up depicted in figure 7 is installed in the Green Energy Park premises of RGTU, Bhopal. After completing the field installation, test runs were conducted in two phases: In the first phase, electrolysis of an aqueous solution of 25% (wt/vol.) KOH was performed under atmospheric pressure for three pairs of austenitic S.S. electrodes (SS310, SS316& SS316L) used sequentially. In this phase, all the three electrodes were used in their original condition (as procured from the market). Inter-electrode spacing of 20.5mm was maintained (keeping in mind the notoriety of gas bubbles at very close electrode spacings) & current density was varied between 0.01A/cm^2 to 0.244A/cm^2. All the test runs were performed under real-time conditions. The cell voltage reading was set to its pre-fixed value for each experiment by manually adjusting the voltage regulator. The corresponding value of the cell current is recorded from the digital ampere meter mounted on the DC-DC converter panel after running the AWE for about 70-90 seconds. After that, the experimental hydrogen gas production rate was measured by the water displacement method using a vertically mounted graduated burette & stopwatch.

The effect of exerting pre-fixed cell voltages on the cell currents, experimental rate of production of hydrogen gas, and the faradic efficiency of the cell for individual sets of S.S. electrodes (normal surface morphology) are measured, recorded & calculated, which is elaborated in the experimental data tables (Table nos.1, 2 & 3).

Table 1. Experimental cell current, hydrogen production rate & faradic efficiency tables for AWE with SS 310 electrodes (normal surface morphology)

S.NO	V cell (V)	I cell (A)	Theoritical H_2 Production rate (gms/mins)	Experimental H_2 Production Rate (gms/mins)		Faradic Efficiency (n Faradic) %
				ml/min	(gms/min)	
1	1.7	0.3	0.00019	-	-	-
2	1.8	1.1	0.000684	5.2	0.00047	68.32
3	1.9	2.2	0.001368	11	0.00099	72.27
4	2	3	0.001866	16	0.00144	77.06
5	2.1	5.1	0.0031715	28	0.00252	79.35
6	2.2	7.4	0.004601	41	0.000369	80.09
7	2.3	9.1	0.005659	51	0.00458	81
8	2.4	11.2	0.006965	63	0.00566	81.29
9	2.5	13.1	0.00815	73	0.00665	81.6
10	2.6	16.2	0.01009	92	0.00827	82.11
11	2.7	18.1	0.01126	104	0.00935	83.01
12	2.8	20.6	0.0128	119	0.01696	83.56
13	2.9	22.1	0.013743	131	0.001177	85.67
14	3	24.7	0.01536	149	0.13392	87.18
15	3.1	26.5	0.01648	161	0.01447	87.8
16	3.2	29.4	0.01828	180	0.01618	88.5
17	3.3	33.6	0.20894	210	0.01887	90.33
18	3.4	36.4	0.022636	231	0.02076	91.72
19	3.5	38.7	0.02407	249	0.02238	92.97

Table 2. Experimental cell current, hydrogen production rate & faradic efficiency tables for the AWE with SS 316 electrodes (normal surface morphology)

S.NO	V cell (V)	I cell (A)	Theoritical H_2 Production rate (gms/mins)	Experimental H_2 Production rate (gms/mins) ml/min (gms/min)	Faradic Efficiency (n Faradic) % -
1	1.7	0.1	0.000622 -	- -	-
2	1.8	0.7	0.000435	3.2 0.0002876	66.11
3	1.9	1.4	0.00087	6.9 0.000621	71.28
4	2	2.1	0.001305	10.5 0.000944	72.31
5	2.1	3.9	0.002425	20 0.001798	74.12
6	2.2	6	0.0037311	31 0.002786	74.67
7	2.3	7.8	0.00485	42 0.00377496	77.83
8	2.4	9.3	0.00578	52 0.00467367	80.86
9	2.5	11.9	0.0074	68 0.0061118	82.59
10	2.6	14.5	0.009017	84 0.00755	83.72
11	2.7	16.2	0.01007	95 0.0085386	84.79
12	2.8	18	0.01119	107 0.009617	85.94
13	2.9	19.9	0.012375	120 0.0107856	87.15
14	3	22.6	0.014054	138 0.01240344	88.2
15	3.1	24.8	0.015422	155 0.0139314	90.33
16	3.2	27.1	0.01685	171 0.015369	91.21
17	3.3	28.9	0.01797	184 0.016538	92.03
18	3.4	32.5	0.02021	209 0.018785	92.94
19	3.5	36.2	0.02251	234 0.021032	93.43

Table 3. Experimental cell current, hydrogen production rate & faradic efficiency tables for the AWE with S.S. 316L electrodes (normal surface morphology)

S.NO	V cell (V)	I cell (A)	Theoritical H_2 Production rate (gms/mins)	Experimental H_2 Production rate (gms/mins) ml/min (gms/min)	Faradic Efficiency (n Faradic) % -
1	1.7	0.13	8.084E-05	- -	-
2	1.8	0.9	0.00056	4.5 0.000404	72.2
3	1.9	1.8	0.00112	9.2 0.000827	73.83
4	2	2.5	0.001555	13 0.00168	75.14
5	2.1	4.8	0.002985	25 0.002247	75.27
6	2.2	6.7	0.004166	35.9 0.00324	77.67
7	2.3	8.4	0.005224	46 0.0041345	79.1
8	2.4	10.2	0.006343	56 0.005033	79.35
9	2.5	12.8	0.00796	72 0.00647	81.29
10	2.6	14.7	0.00914	85 0.00764	83.5
11	2.7	16.5	0.01026	96 0.00863	84.1
12	2.8	18.2	0.01132	108 0.00971	85.7
13	2.9	20.3	0.01262	121 0.01088	86.17
14	3	23.8	0.0148	148 0.013302	89.8
15	3.1	25.5	0.01586	160 0.01438	90.7
16	3.2	27.9	0.01735	176 0.015819	91.17
17	3.3	30	0.01866	191 0.01747	92
18	3.4	33.6	0.02089	216 0.01941	92.93
19	3.5	36.8	0.02288	237 0.021032	93.1

The V-I curves of the AWE portraying the variation in the cell currents upon applying the pre-fixed cell voltages for the individual electrodes are drawn. The dependence of the experimental rate of hydrogen production($m_{H2(exp.)}$) on the applied cell voltage(V_{cell}) for the individual electrode sets is illustrated in the experimental hydrogen production rate($m_{H2(exp.)}$) versus cell voltage (V_{cell})curves. Calculations for the theoretical rate of hydrogen production & the faradic efficiency were performed according to the following formulae [26]:

$$m_{H2(theo.)}=\frac{n\times I_{cell}}{F}\times 60 \text{ gms/min.} \quad (1)$$

Where,
n= No. of cells (n=1 in this case)
I_{cell} = Cell current in Amps.
F= Faraday's constant (96,495 Coulombs/mol.)

$$\text{Faradic efficiency } (\eta_F)\ \% = m_{H2(exp.)}/m_{H2(theo.)} \quad (2)$$

For the second phase of experiments, the electrodes' surface morphology is modified to increase the effective surface area of the electrodes[23]. It is achieved by polishing the three-electrode pairs in a criss-cross pattern with emery paper of P400 grade[23]. In this phase, the experimental test runs performed in the previous phase are repeated for the same input process variables (i.e., same pre-fixed sets of cell voltages & % KOH concentration) but with electrodes (SS310, SS316 & SS316L, respectively) having modified surface morphology. Cell currents and experimental hydrogen production rates for each pre-defined value of applied cell voltage are measured, noted down & corresponding values for $m_{H2(theo.)}$ & η_F are calculated from eq. 1 & 2(data tables no. 4, 5 & 6).

Table 4. Experimental cell current, hydrogen production rate & faradic efficiency tables for the AWE with SS 310 electrodes (modified surface morphology)

S.NO	V cell (V)	I cell (A)	Theoritical H_2 Production rate (gms/mins)	Experimental H_2 Production rate (gms/mins)		Faradic Efficiency (n Faradic) %
				ml/min	(gms/min)	-
1	1.7	0.5	0.000311	-	-	-
2	1.8	1.25	0.000777	6.2	0.000557256	71.7
3	1.9	3	0.0018656	15.5	0.00139314	74.6
4	2	4.3	0.002674	23	0.00206724	77.31
5	2.1	6.5	0.004042	36	0.00323568	80.05
6	2.2	9.25	0.005752	52	0.00467376	81.25
7	2.3	11.2	0.006965	64	0.00575232	82.58
8	2.4	13.5	0.008395	78	0.00701064	83.51
9	2.5	16	0.0099497	94	0.00844872	84.91
10	2.6	18.7	0.011629	111	0.00997668	85.79
11	2.7	21	0.013059	126	0.1132488	86.72
12	2.8	23	0.014303	139	0.01249332	87.34
13	2.9	25.5	0.0158574	155	0.0139314	87.85
14	3	28.5	0.017723	176	0.01581888	89.25
15	3.1	31	0.019278	195	0.0175266	90.91
16	3.2	34.5	0.021454	219	0.01968372	91.74
17	3.3	37.4	0.023258	239	0.02148132	92.36
18	3.4	40	0.0248743	258	0.02318904	93.22
19	3.5	43.7	0.027175	285	0.0256158	94.26

Table 5. Experimental cell current, hydrogen production rate & faradic efficiency tables for the AWE with SS 316 electrodes (modified surface morphology)

S.NO	V cell (V)	I cell (A)	Theoritical H_2 Production rate (gms/mins)	Experimental H_2 Production rate (gms/mins)		Faradic Efficiency (n Faradic) %
				ml/min	(gms/min)	-
1	1.7	0.2	0.000124	-	-	-
2	1.8	1.5	0.000933	7	0.000629	67.4
3	1.9	1.9	0.001182	9.7	0.000872	73.8
4	2	2.7	0.00168	14	0.001258	75
5	2.1	4.5	0.002798	24	0.002157	77.09
6	2.2	6.7	0.00417	36.5	0.00328	78.7
7	2.3	8.8	0.005472	49.3	0.004311	80.9
8	2.4	11.1	0.0069	62.5	0.00562	81.4
9	2.5	13.6	0.008427	78	0.007011	82.8
10	2.6	15.3	0.00951	89	0.007999	84.11
11	2.7	17.8	0.01107	105	0.009437	85.3
12	2.8	20.3	0.01262	122	0.010965	86.8
13	2.9	22.1	0.01374	133	0.011954	87
14	3	24.6	0.015298	150	0.013482	88.1
15	3.1	26.5	0.01648	164	0.01474	89.44
16	3.2	29.4	0.018283	184.5	0.0165828	90.7
17	3.3	32.2	0.020024	207	0.0186051	92.9
18	3.4	36.3	0.02257	235	0.0211218	93.58
19	3.5	40.5	0.02518	264	0.023728	94.23

Table 6. Experimental cell current, hydrogen production rate & faradic efficiency tables for the AWE with S.S. 316L electrodes- (modified surface morphology)

S.NO	V cell (V)	I cell (A)	Theoritical H_2 Production rate (gms/mins)	Experimental H_2 Production rate (gms/mins)		Faradic Efficiency (n Faradic) %
				ml/min	(gms/min)	-
1	1.7	0.2	0.0001244	-	-	-
2	1.8	1.7	0.00106	8.6	0.000773	72.9
3	1.9	2.4	0.0015	12.7	0.0011415	76.09
4	2	2.9	0.0018	15.5	0.00139	77.3
5	2.1	5.7	0.003545	31	0.002786	78.59
6	2.2	7	0.00566	39.5	0.00355	81.61
7	2.3	9.1	0.00721	52	0.00464	82.57
8	2.4	11.6	0.0069	67	0.006022	83.5
9	2.5	13.7	0.00852	80	0.00719	84.39
10	2.6	16.2	0.01007	96	0.00863	85.68
11	2.7	17.6	0.010945	106	0.00953	87.04
12	2.8	21	0.01306	128	0.011505	88.09
13	2.9	23	0.0143	141	0.012673	88.62
14	3	24.9	0.0155	154	0.01384	89.3
15	3.1	27	0.01679	169	0.0151897	90.46
16	3.2	29.9	0.01859	190	0.0170772	91.86
17	3.3	32.7	0.020335	208	0.018695	91.93
18	3.4	37	0.02301	237	0.0213016	92.57
19	3.5	41.1	0.02556	268	0.024087	94.24

V-I curves for the AWE are drawn for the three sets of S.S. electrodes and compared with their respective normal surface geometry versions (fig.8,9 & 10). The V-I curves for the three S.S. electrode specimens with only modified surface geometry are also compared (fig.11). Similarly, the $m_{H2(exp.)}$ versus V_{cell} curves are also drawn and compared for each electrode pair(fig.12-15). As the cell voltage qualitatively represents the electric power consumed to produce a certain mass flux of hydrogen, attaining higher cell currents for lower values of cell voltages reflects higher hydrogen production efficiency [20].

A detailed analysis of these performance comparisons is conducted in section 4 of the paper.

4. Results and Discussions

In this section, the influence of surface morphology of three sets of austenitic S.S. electrodes (SS310, SS316 & SS316L) on the electric power consumption & the rate of hydrogen production of the PV-AWE under examination is studied and analyzed. The polarization curves and experimental hydrogen production rate ($m_{H2(exp.)}$) versus cell voltage (V_{cell})curves for the individual electrode sets with normal and modified surface morphologies are drawn & compared.

Comparing these cell polarization curves for the three sets of electrodes (plane & modified morphology) indicates an improvement in the values of cell currents for the electrodes with modified morphology over their respective normal surface geometry versions (fig.8-10). This rise in the cell current for the S.S. electrodes can be attributed to the increase in the electrodes' active surface area, which results in the decrease in the overpotential. The results are in conformance/agreement with the studies conducted by Lavorante et al. [19] & Zeng et al. [23].

However, it is observed that SS310 electrodes portray distinctly higher values of cell currents compared to SS316 & SS316L electrode samples which show comparable values for I_{cell}(fig. 11)

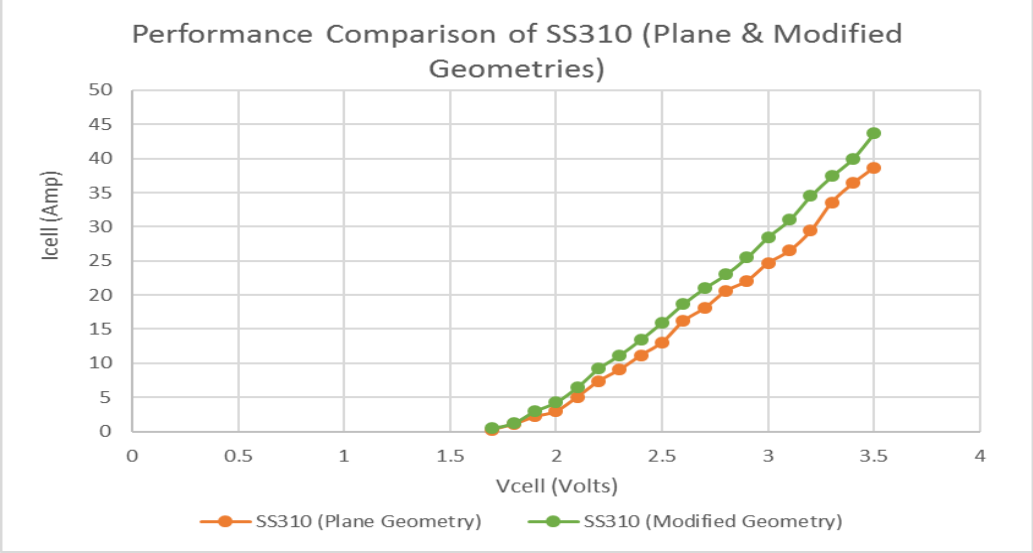

Fig. 8 Performance Comparison of SS310 (Plane & Modified Geometries)

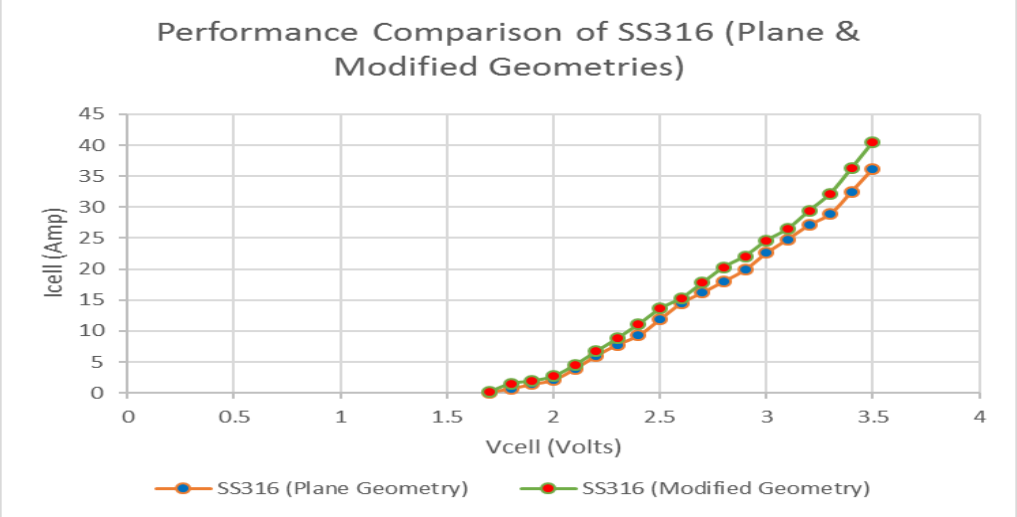

Fig. 9 Performance Comparison of SS316 (Plane & Modified Geometries)

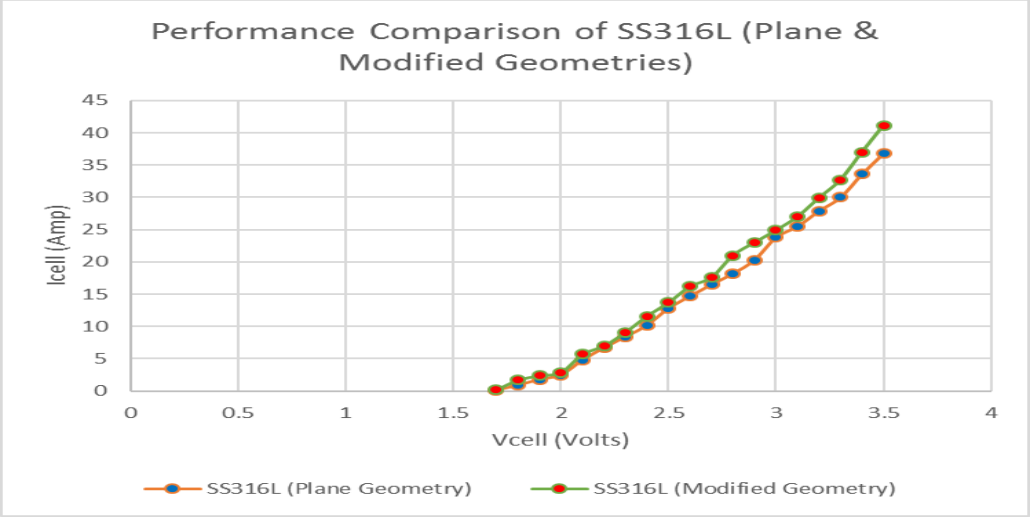

Fig. 10 Performance Comparison of SS316L (Plane & Modified Geometries)

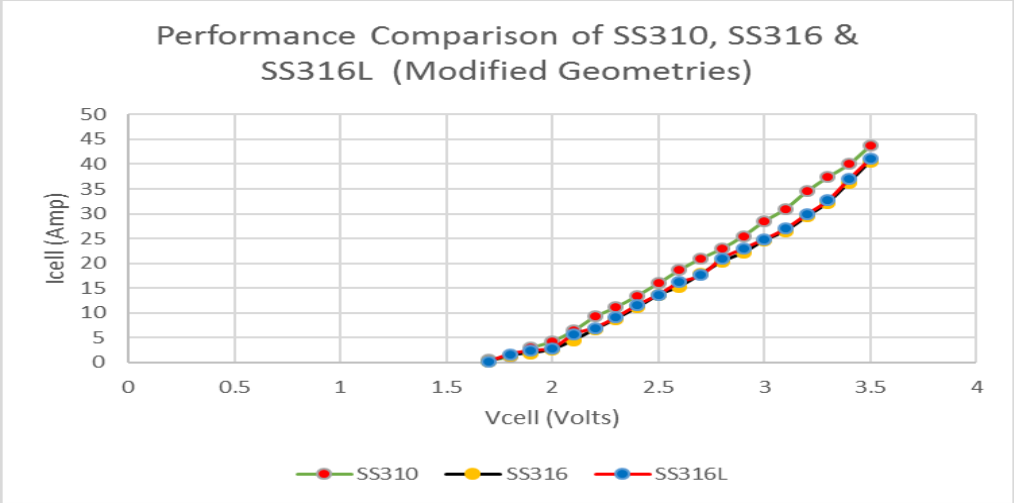

Fig. 11 Performance Comparison of SS310, SS316 & SS316L (Modified Geometries)

Improvement in the cell current values for the three S.S. electrodes with modified morphology also results in improved experimental hydrogen production rate as illustrated in graphs (fig. 12-14).

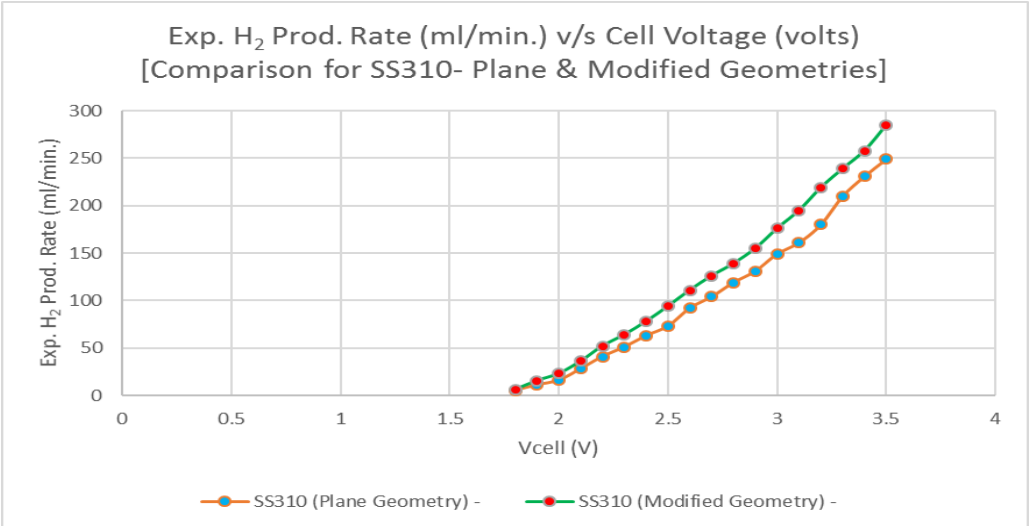

Fig. 12 Exp. H_2 Prod. Rate (ml/min.) v/s Cell Voltage (volts) [Comparison for SS310- Plane & Modified Geometries]

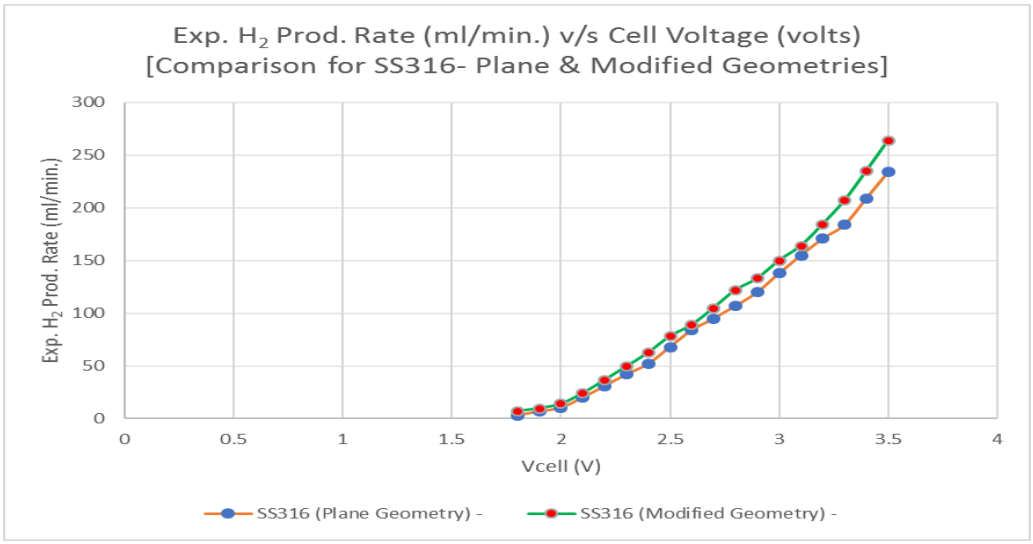

Fig. 13 Exp. H_2 Prod. Rate (ml/min.) v/s Cell Voltage (volts) [Comparison for SS316- Plane & Modified Geometries]

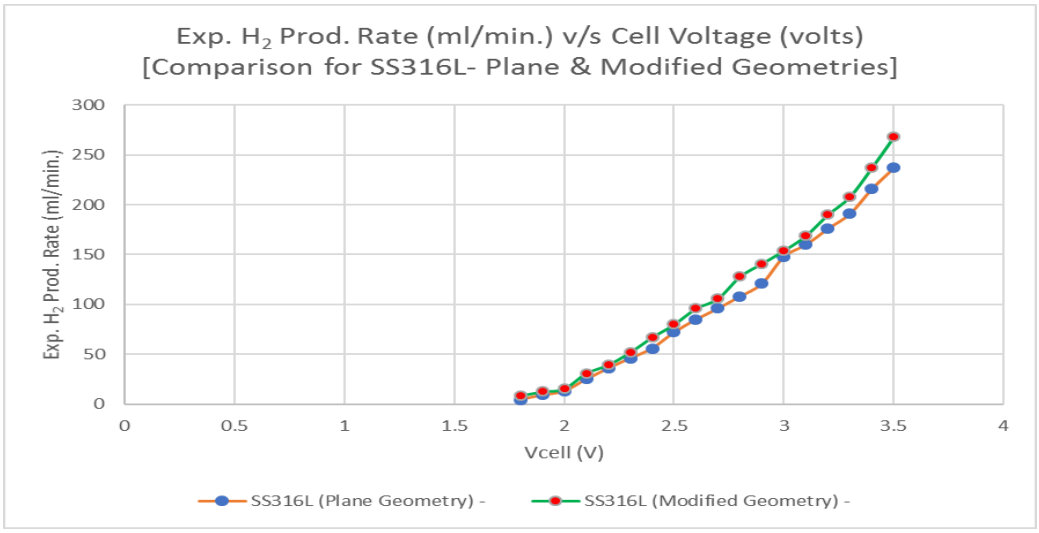

Fig. 14 Exp. H_2 Prod. Rate (ml/min.) v/s Cell Voltage (volts) [Comparison for SS316L- Plane & Modified Geometries]

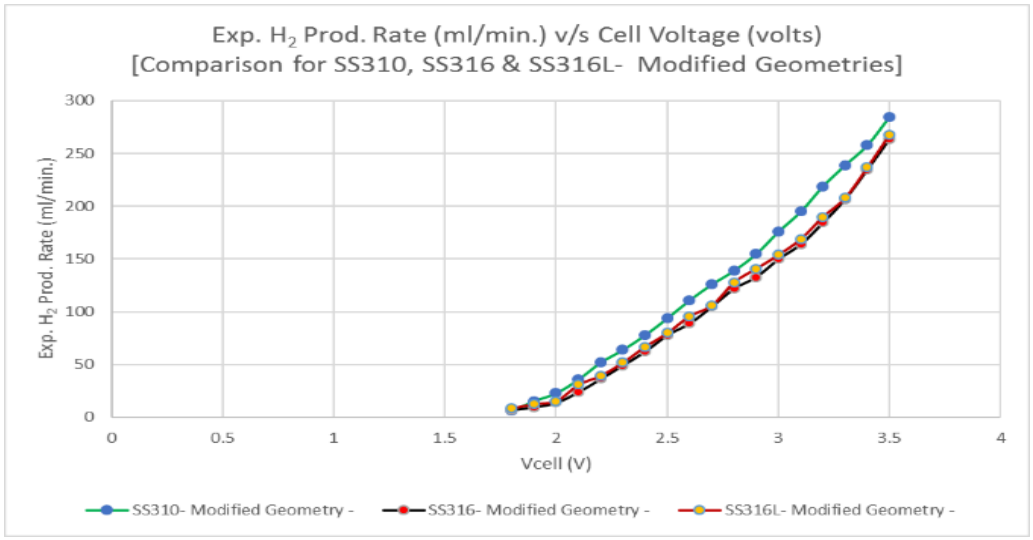

Fig. 15 Exp. H_2 Prod. Rate (ml/min.) v/s Cell Voltage (volts) [Comparison for SS310, SS316 & SS316L-Modified Geometries]

Comparison of the $m_{H2(exp.)}$ vs V_{cell} curves for the three austenitic S.S. electrode samples (with only modified surface morphology) also reveals that SS310 electrode outperforms the other two S.S. electrode specimens(fig.15).

The accumulation of gas bubbles observed at the electrolyte-electrode interface, particularly at higher values of current densities causes a short termed but sustained fluctuation in the cell current values before it attains stability. At higher current densities, large diameter gas bubbles cling to the electrode surface thus isolating their active sites from the reaction ions. This phenomenon, known as bubble effect leads to high over potential and large ohmic voltage drop[10,11].

5. Conclusion

Surface modification improves the values of cell current densities for pre-fixed values of cell voltages. Therefore, the experimental mass rate of hydrogen production also gets improved. However, among the three austenitic S.S. electrode samples used in this experimental study, SS310 electrode shows noticeably better values of cell currents compared to SS316 & SS316L electrode samples both for normal and modified surface morphologies. It can be attributed to the higher % composition of nickel in SS310.

The bubble phenomenon (specifically for higher cell current densities) results in the rise of the ohmic resistance of the electrolytic bath and is thus detrimental to the cell performance. Implementation of suitable mechanisms for timely elimination of the accumulated gas bubbles from the electrode surfaces can lead to further improvement in the AWE performance, which can be a potential area for future research.

References

[1] M. Mori, T. Mrzljak, B. Drobnic and M. Sekavcnik., Integral characteristics of hydrogen production in alkaline electrolyzers, Journal of Mechanical Engg.,59(10) (2013) 585-594.

[2] R. Garcia-Valvarde, N. Espinosa and A. Urbina., Optimized method for photovoltaic-water electrolyzer direct coupling, Int. J. Hydrogen Energy, 36(2011) 10574-10586.

[3] H. Steeb, A. Mehrmann, W. Seeger, and W. Schnurnberger., Solar Hydrogen Production: Photovoltaic/ Electrolyzer System with Active Power Conditioning, Int. J. Hydrogen energy, 10(6)(1985) 353-358.

[4] M. Vanags, J. Kleperis, G. Bajars and A. Lusis., Water electrolysis using electrodes with modified surface/volume, Journal of Physics, Conference series on functional materials and nanotechnologies, (2007) 1-7.

[5] M. Bodner, Astrid Hofer and Victor Hacker., Hydrogen generation from alkaline electrolyzer: Advanced Review, WIREs Energy Environment, John Wiley and Sons Ltd ,(2014).

[6] F. Barbir and T. N. Veziroglu., Hydrogen economy: Status and outlook, 1st International Conference on Energy Efficiency and Conservation. Hong Kong. 15th-17th Jan. (2003) 34-39.

[7] C. K. Kjartansdottir, L. P. Nielsen and P. Moller., development of durable and efficient electrodes for large scale alkaline water electrolysis. Int. J. Hydrogen Energy, 38(2013)8221-8231.

[8] A. Ursua, L.M. Gandia and P. Sanchis.,Hydrogen production from water electrolysis: Current status and future trends, Invited paper, Proceedings of the IEEE, 100(2)(2012)410-426.

[9] D.M.F. Santos, C. Sequeira and J.L. Figueiredo., Hydrogen production from alkaline water electrolysis, Quimica Nova, 36(8) (2013) 1-33.

[10] K. Zeng and D. Zhang., Recent progress in alkaline water electrolysis for hydrogen production and applications, Progress in Energy and Combustion Science, 36(3)(2010)307-326.

[11] M. Wang, Z. Wang, X. Gong and Z. Guo., The intensification technologies to water electrolysis for hydrogen production-A review. Renewable and Sustainable Energy Reviews, 29 (2014) 573-578.

[12] G.Saur., Wind-to-Hydrogen- Project: Electrolyzer capital cost study. Technical report, NREL, (2008).

[13] M. H. Sellami and K. Loudiyi., Electrolytes behavior during hydrogen production by solar energy, Renewable &Sustainable Energy Reviews, 70 (2017) 1331-1335.

[14] F. Chakik, M. Kaddami and M. Mikou., Effect of operating parameters on hydrogen production by electrolysis of water, Int. J. Hydrogen Energy, 42 (2017)25550-25557.

[15] J.M. O-Ramirez, M.L. Campos-Cornelio, J. Godinez, E. Borja-Arco and R.H. Castellanos., Studies on the hydrogen evolution reactions on different stainless steels, Int. J. Hydrogen Energy 32(2007) 3170-3173.

[16] A.N. Colli, H. Girault and A. Battistel., Non precious electrodes for practical alkaline water electrolysis. Materials, MDPI, 12(2019) 1336.

[17] E. Nassar and A. Nassar., Corrosion behavior of some conventional steels at different temperatures in the electrolyzing process. Energy Procedia,93 (2016) 102-107.

[18] R. L. Le Roy., Industrial water electrolysis: Present & future, Int. J. Hydrogen Energy, 8(6) (1983), 401-417.

[19] M. J. Lavorante, C. Reynoso and J. Franco., Straight parallel electrodes and variable gap for hydrogen and oxygen evolution reactions. Int. J. Electrochemistry, (2019) 1-11.

[20] N. Nagai, M. Takeuchi, T. Kimura and T. Oka., Existence of optimum space between electrodes on hydrogen production by water electrolysis, Int. J. Hydrogen Energy, 28(2003) 35-41.

[21] A. Dukic and M. Firak., Hydrogen production using alkaline electrolyzer and P.V. module. Int. J. Hydrogen Energy, 36 (2011) 7799-7806.

[22] V. Nikolic, G. Tasic, A. Maksic, D. Saponjic, S. Miulovic and M. Kaninski., Raising hydrogen generation efficiency from alkaline water electrolysis- Energy saving. Int. J. Hydrogen Energy, 35 (2010) 12369-12373.

[23] K. Zeng and D.Zhang., Evaluating the effect of surface modifications on Ni based electrodes for alkaline water electrolysis. Fuel, 116(2014) 692-698.

[24] S.K.Mazloomi and N.Sulaiman., Influencing factors of water electrolysis electrical efficiency, Renewable and Sustainable Energy Reviews, 16 (2012) 4257-4263.
[25] T. L. Gibson and N.A. Kelly., Optimizationof solar powered hydrogen production using photovoltaic electrolysis devices. Int. J. Hydrogen Energy, 33(2008) 5931-5940.
[26] B. Paul, Direct coupling of the photovoltaic array and PEM electrolyzer in solar hydrogen systems for remote area power supply", Ph.D. dissertation, School of Aerospace, Mechanical & Manufacturing Engg, RMIT University. Australia, (2009).